Solid-State Electronics 199 (2023) 108503

Contents lists available at ScienceDirect

Solid State Electronics

journal homepage: www.elsevier.com/locate/sse

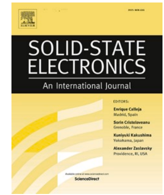

Analysis of uniaxial stress impact on drift velocity of 4H-SiC by full-band Monte Carlo simulation

T. Nishimura *, K. Eikyu, K. Sonoda, T. Ogata

Renesas Electronics Corporation, 751, Horiguchi, Hitachinaka, Ibaraki 312-8511, Japan

ARTICLE INFO

The review of this paper was arranged by "Francisco Gamiz"

Keywords:
Power semiconductor
SiC
First principles calculation
Full-band Monte Carlo simulation

ABSTRACT

SiC is expected to be the next-generation semiconductor material especially for power devices, and some have been put into practical use. However, its stress response has not been completely elucidated. In this paper, we analyzed the stress response of the drift velocity of 4H-SiC with a combination of first principles calculation and full-band Monte Carlo simulation. The response decreases with an increase in the electric field except for a hump around 1 MV/cm. The decreasing trend is explained by increasing scattering rates which diminish the effect of the change of the effective mass due to stress. The hump comes from the transition of electrons to band minima with a lighter effective mass.

1. Introduction

In recent years, the demand for semiconductor devices capable of highly efficient power control has been increasing due to the electrification of automobiles and the increase in the amount of communication in data centers. However, conventional Si power devices have reached the limit of performance due to their material properties, and it is difficult to dramatically improve their performance. So, next-generation power materials such as SiC, GaN and GaO are attracting attention because these materials have wide bandgap and higher dielectric breakdown electric field than Si and enhance the performance of power semiconductor device.

To accurately reproduce the electron transport in a power device, the conventional simulation method considering only the band bottom is not sufficient. It is because under a high electric field, electrons transit to a higher band. So full-band Monte Carlo (FBMC) simulation is effective. There are many reports of analyzing the electron transport in SiC by FBMC simulation [1,2], but few have considered the effects of stress. Therefore, we have recently reported the FBMC analysis of the stress response of 4H-SiC in the c-axis direction [3] where the stress dependence of the impact ionization coefficient is small, and the drift velocity is positively correlated with the tensile stress. In this paper, we analyze the stress response of the drift velocity in more detail by observing the distribution of electrons in the band structure.

2. Method

We use first principles calculations and FBMC simulations to analyze the stress response of 4H-SiC. The band structure of 4H-SiC used in this paper is calculated by the first-principles calculation tool DMol3 based on the density functional theory (DFT) [4]. The functional used for the calculation is GGA-PBE [5] and k-point is set to 30x30x10 in each of the a-, b-, and c-axes of 4H-SiC. Since it is well known that DFT tends to underestimate the bandgap and the curvature of bands, the band structure near the conduction band bottom is calibrated to match the calculation results of the high-precision first-principles calculation tool ecalj based on a quasiparticle self-consistent GW (QSGW) method [6,7]. The QSGW method shows higher accuracy than the one-shot GW method [8]. It has been also reported that FBMC simulations using the band structure calculated by the QSGW method reproduce measured data of the electric-field dependence of the impact ionization coefficient with high accuracy [2]. We have confirmed that the calibrated band structure is almost the same as that obtained by QSGW method up to the high energy band of about 10 eV from conduction band bottom as shown in Fig. 1. This is a sufficient range to consider the electron transport under a high electric field.

Then band calculation is performed on the assumption that uniaxial stress is applied along the c-axis. The lattice deformation was calculated according to Young's modulus and Poisson's ratio, which are set to be 400 GPa and 0.16 respectively. The band structure simulated by the first-principles calculation is input to the FBMC simulator.

* Corresponding author.
E-mail address: tomoya.nishimura.uf@renesas.com (T. Nishimura).

https://doi.org/10.1016/j.sse.2022.108503

Available online 4 November 2022
0038-1101/© 2022 Elsevier Ltd. All rights reserved.

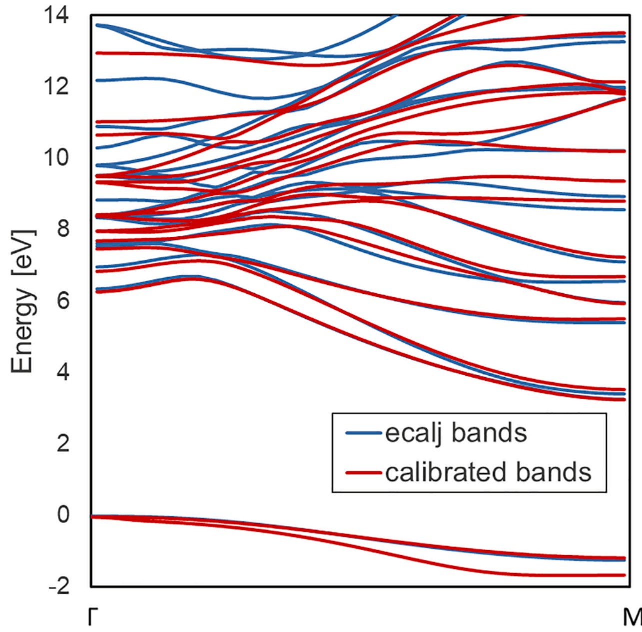

Fig. 1. Comparison of calibrated band structure and ecalj band structure.

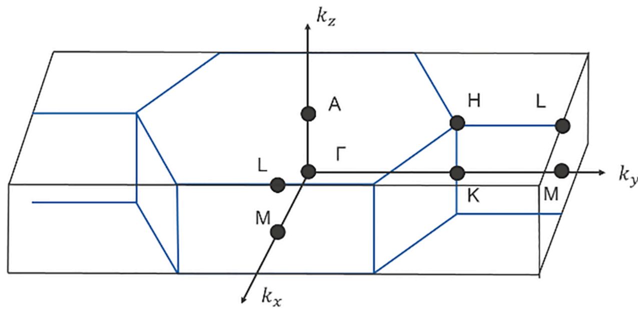

Fig. 2. FBMC simulation domain which contains double Brillouin zone of 4H-SiC.

The FBMC simulator used to derive the stress response of the drift velocity includes scattering mechanisms such as acoustic phonon scattering, non-polar optical phonon scattering, and impact ionization. Acoustic phonon scattering rate and non-polar optical phonon scattering rate are given as a function of carrier energy. The impact ionization rate is calculated through the QSGW method and implemented into the FBMC simulator as a function of the electron energy. In this paper, those scattering rates are calibrated to non-stressed 4H-SiC. Therefore, it should be noted that the change of the scattering rates due to the stress is not considered [9].

A double Brillouin zone is adopted for the simulation domain in k-space which enables to use an orthogonal k-space mesh and simple boundary condition (Fig. 2).

The details of the simulation parameters and calibration are reported elsewhere [2,3].

3. Results and discussion

Fig. 3 shows the c-axis stress dependence of the band structure of 4H SiC by first principles calculations. The curvature of the conduction band bottom (M-point) decreases under compressive stress and increase under tensile stress. This indicates that the electron mobility of 4H-SiC under a low electric field improves with tensile stress. The bandgap shows a monotonous decrease in the range of −6 GPa to +10 GPa but decreases slightly for compressive stresses exceeding −6 GPa.

Next, the electric-field dependence of the electron drift velocity calculated by FBMC simulation is shown in Fig. 4. Here the electric-field is applied along the c-axis, which is parallel to the stress application direction. At low electric fields, the drift velocity is proportional to the electric field, but after peaking once, it decreases at high electric fields. This can be explained by the band population. At low electric fields, the electrons are localized at the M- point of the conduction band bottom as shown in Fig. 5, while at high electric fields, they transit to other valleys where electrons have a heavier effective mass than M-point. Therefore, the stress dependence of the drift velocity at a low electric field is mostly corresponding to the curvature change at M-point (Fig. 6). In addition, the fact that the absolute value of the drift velocity is larger under tensile stress at a low electric field is consistent with the tendency of the curvature change at M-point shown in Fig. 3.

Next, stress sensitivity coefficient of the drift velocity γ defined below is plotted against applied electric field in Fig. 7. γ is defined by the following formula

$$\gamma = \frac{\Delta V_d / V_{d0}}{\Delta \sigma}$$

where ΔV_d and $\Delta\sigma$ are the difference of the drift velocity and the applied stress, respectively and V_{d0} is the drift velocity of unstressed 4H-SiC. The three lines in Fig. 7 show the same tendency with the electric field. Therefore, we discuss the sensitivity between 0 GPa and 10 GPa.

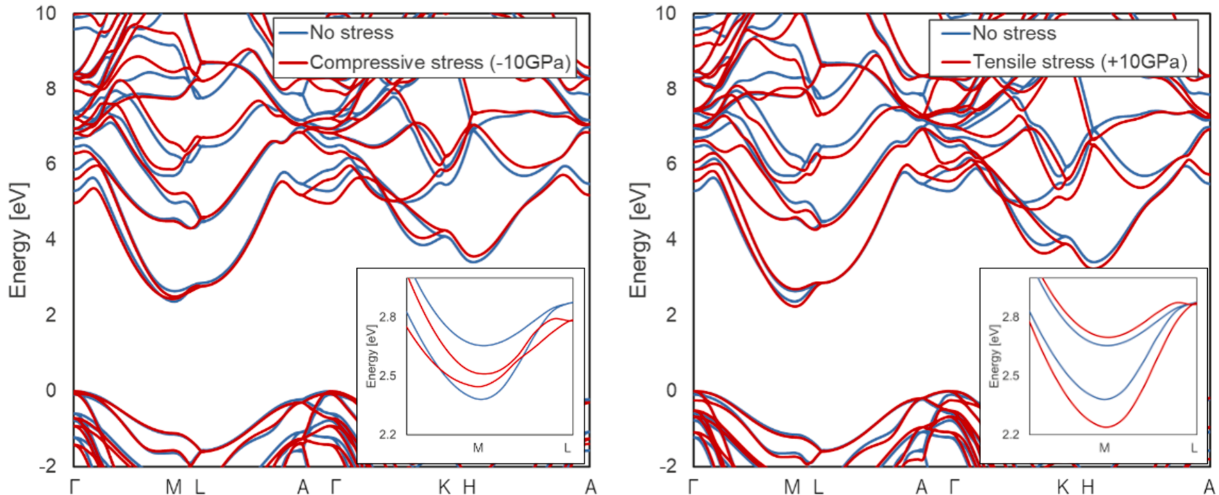

Fig. 3. Band structure change when c-axis stress is applied. The valence band top is set to 0 eV. (L) compressive stress applied, (R) tensile stress applied.

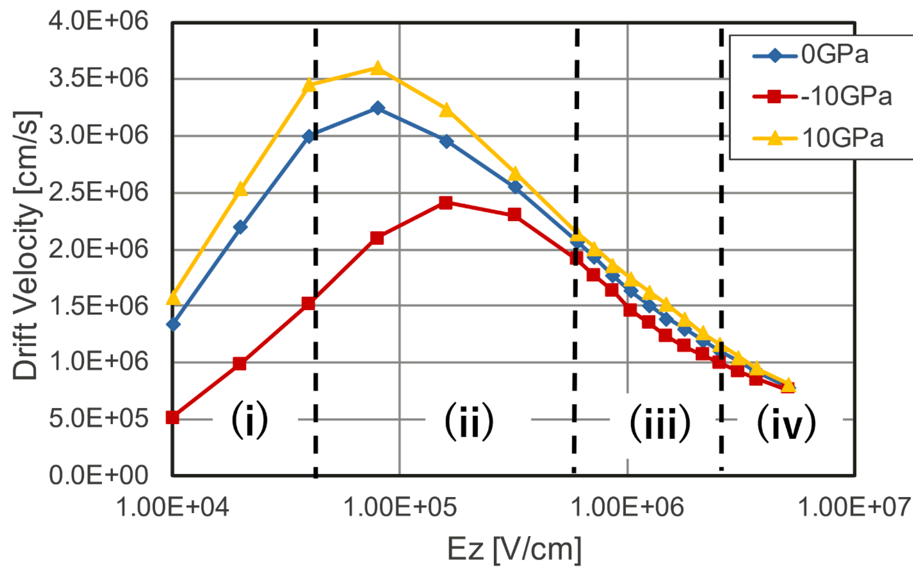

Fig. 4. Electric-field dependence of drift velocity.

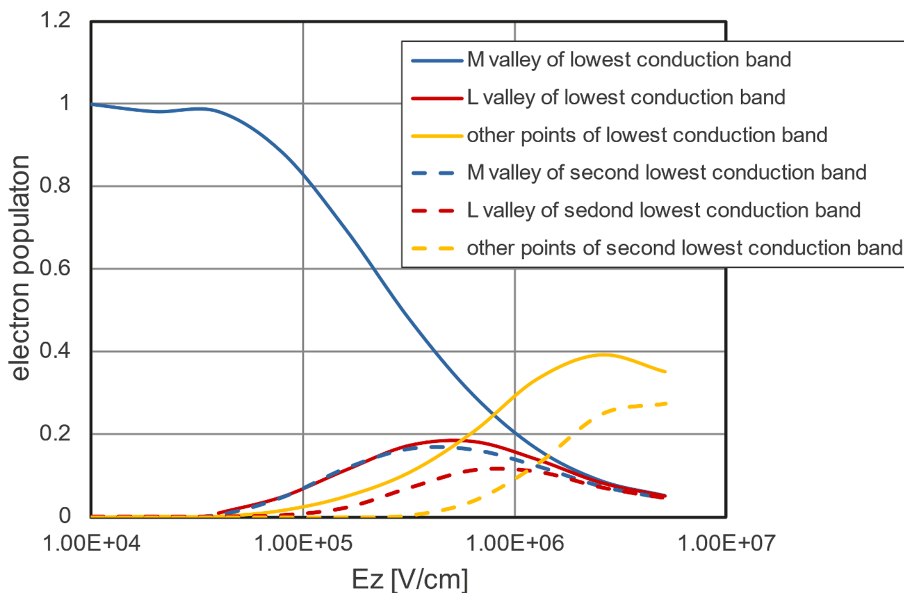

Fig. 5. Electron population in each band @ σ = 0 GPa.

In the low electric-field region (i), the electrons are localized at M-point and γ corresponds mostly to the change of the effective mass or M-valley curvature. Furthermore, in the region (ii) where the electric field becomes higher, the influence of the scatterings become larger, so that γ becomes smaller.

An interesting feature is the peak appearing in the region (iii) around 1 MV/cm. This indicates that the decrease in the drift velocity at a high electric field is gentler when tensile stress is applied. It can be explained by a modulation of intervalley transfer [10] by the tensile stress. The electron population in each band is shown in Figs. 8 and 9. The display area in Fig. 9 is the double Brillouin zones, which is the same as the calculation domain of the simulator. Under no stress, the electrons localized near the M-valley transit to the L-point or higher bands as the electric field increases. On the other hand, when tensile stress is applied, there are fewer electrons that transit to the L-point and higher bands, and more electrons transit to the H-point instead. So, the decrease in the drift velocity is alleviated since the effective mass of the electron located at the H-point is smaller than the one at the L-point or the higher band (Figs. 6, 10). Furthermore, the cause of such a difference in band transition is explained by a change of the band structure when stress is applied. Under tensile stress, the energy difference between M-point and L-point of the lowest conduction band and that between the lowest and the second lowest conduction band become wider. On the other hand, the energy difference from M-point to H-point slightly shrinks as shown Fig. 3 and Table 1. Therefore, it is considered that electrons are likely to transit to the H-point under tensile stress.

Furthermore, in the region (iv) of Fig. 4 where the effect of scattering becomes even greater, the stress sensitivity γ of the drift velocity difference becomes smaller.

4. Conclusion

The drift velocity and its stress response in low electric fields strongly depend on the curvature at the M-point. The drift velocity becomes larger by tensile stress due to the change in the curvature under the assumption that the scattering rate does not change with stress. This

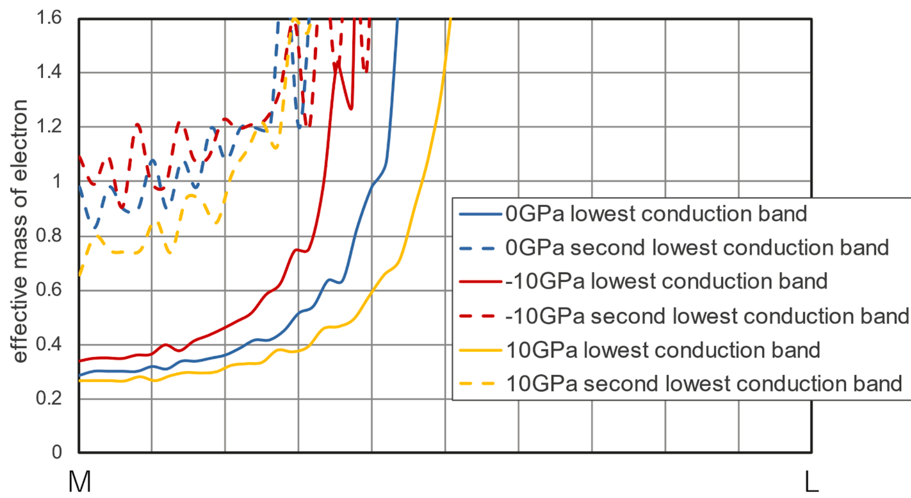

Fig. 6. Electron effective mass in M valley.

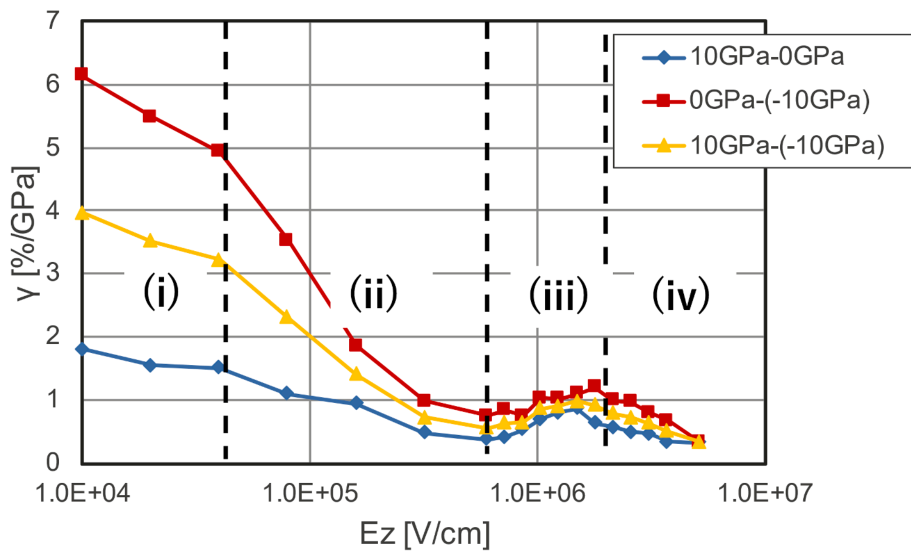

Fig. 7. Stress sensitivity of drift velocity.

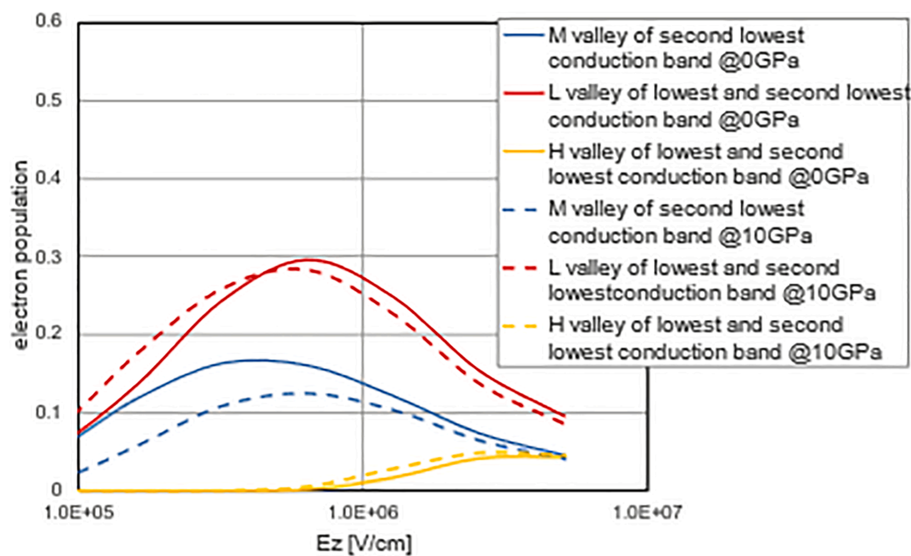

Fig. 8. Electron population in M-, L-, and H-valleys.

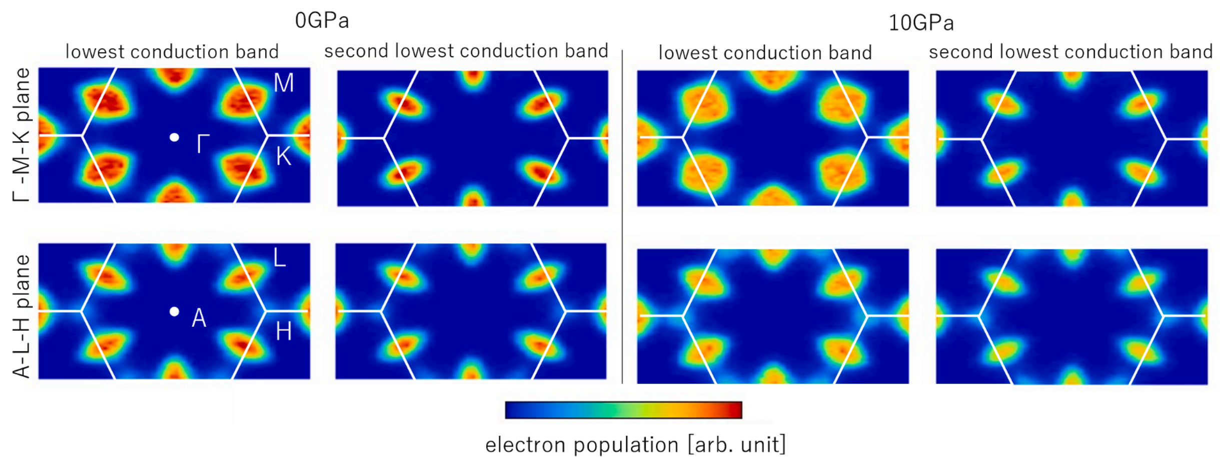

Fig. 9. Electron population in k-space @ Ez = 1.28 MV/cm.

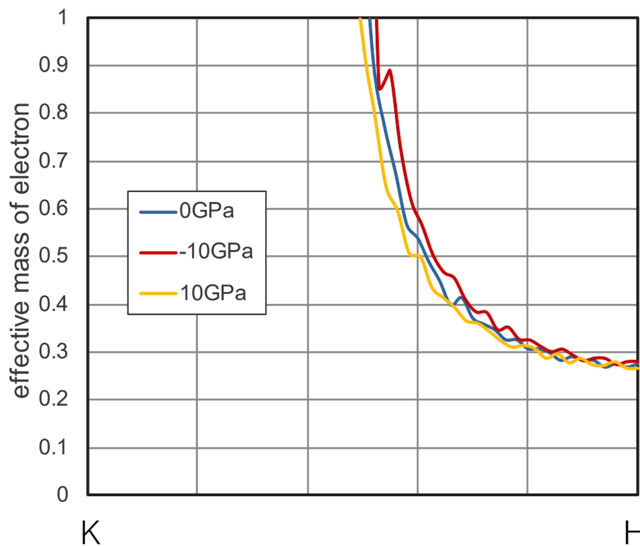

Fig. 10. Electron effective mass in H valley of the lowest conduction band.

Table 1
Electron energy difference of each point. E_{Mo} and E_{M1} are the energy of M-point of the lowest conduction band and second lowest conduction band respectively, E_{Lo} and E_{Ho} are the energy of L-point and H-point of the lowest conduction band respectively.

	$E_{M1} - E_{M0}$	$E_{L0} - E_{M0}$	$E_{H0} - E_{M0}$
unstressed (0GPa)	0.27 eV	0.49 eV	1.04 eV
tensile (10GPa)	0.46 eV	0.63 eV	1.00 eV

result suggests the stress engineering can reduce the on-resistance of the device. In high electric fields the response becomes small due to the scatterings. However around 1 MV/cm, the stress response slightly increases due to the modulation of intervalley transfer.

Declaration of Competing Interest

The authors declare that they have no known competing financial interests or personal relationships that could have appeared to influence the work reported in this paper.

Data availability

The data that has been used is confidential.

Acknowledgment

The authors would like to thank Prof. Y. Kamakura of Osaka Institute of Technology for helpful discussion.

References

[1] A Akturk, N Goldsman, S Potbhare, A Leis. High field density functional theory-based Monte Carlo. 4H-SiC impact ionization and velocity saturation. J Appl Phys. 2009; 105: 033703-1–033703-7. 10.1063/1.3074107.
[2] R Fujita, K Konaga, Y Ueoka, Y Kamakura, N Mori, T Kotani. Analysis of Anisotropic Ionization Coefficient in Bulk 4H-SiC with Full-Band Monte Carlo Simulation. in Proc. of SISPAD. 2017; 289-292. 10.23919/SISPAD.2017.8085321.
[3] T Nishimura, K Eikyu, K Sonoda T. Ogata. Full band Monte Carlo analysis of the uniaxial stress impact on 4H-SiC high energy transport. in Proc of SISPAD. 2021; 28. 10.1109/SISPAD54002.2021.9592533.
[4] BIOVIA Materials Studio DMol3 2019 User Manual.
[5] Perdew J, Burke K, Ernzerhof M. Generalized gradient approximation made simple. Phys Rev Lett 1996;77:3865. https://doi.org/10.1103/PhysRevLett.78.1396.
[6] T Kotani. Quasiparticle self-consistent GW method based on the augmented plane-wave and muffin-tin orbital method. J Phys Soc Jpn 2014; 83: 0974711-1–0974711-11. 10.7566/JPSJ.83.094711.
[7] Deguchi D, Sato K, Kino H, Kotani T. Accurate energy bands calculated by the hybrid quasiparticle self-consistent GW method implemented in the ecalj package. Jpn J Appl Phys 2016;55:051201.
[8] van Schilfgaarde M, Kotani T, Faleev S. Quasiparticle self-consistent GW theory. Phys Rev Lett 2006;96:226402. https://doi.org/10.1103/PhysRevLett.96.226402.
[9] Dhar S, Ungersböck E, Kosina H, Grasser T, Selberherr S. Electron mobility model for <110> stressed silicon including strain-dependent mass. IEEE Trans Nanotechnol 2007;6:97. https://doi.org/10.1109/TNANO.2006.888533.
[10] Butcher PN, Fawcett W. Proc Phys Soc 1965;86:1205.